

■ Ferromagnetic Interactions

Does the Sign of the Cu–Gd Magnetic Interaction Depend on the Number of Atoms in the Bridge?

Jean-Pierre Costes,^{*[a, b]} Carine Duhayon,^[a, b] Sonia Mallet-Ladeira,^[a, b] Sergiu Shova,^[a, b, c] and Laure Vendier^[a, b]*Dedicated to Professor Dante Gatteschi*

Abstract: Several theoretical investigations with CASSCF methods confirm that the magnetic behavior of Cu–Gd complexes can only be reproduced if the 5d Gd orbitals are included in the active space. These orbitals, expected to be unoccupied, do present a low spin density, which is mainly due to a spin polarization effect. This theory is strengthened by the experimental results reported herein. We demonstrate that Cu–Gd complexes characterized by Cu–Gd interactions through single-oxygen and three-atom bridges consisting of oxygen, carbon, and nitrogen atoms, present weak

ferromagnetic exchange interactions, whereas complexes with bridges made of two atoms, such as the nitrogen–oxygen oximate bridge, are subject to weak antiferromagnetic exchange interactions. Therefore, a bridge with an odd number of atoms induces a weak ferromagnetic exchange interaction, whereas a bridge with an even number of atoms supports a weak antiferromagnetic exchange interaction, as observed in pure organic compounds and also, as in this case, in metal–organic compounds with an active spin polarization effect.

Introduction

Since the discovery of ferromagnetic Cu–Gd interactions in a trinuclear Cu–Gd–Cu complex^[1] a lot of studies aimed at evaluating the nature and magnitude of the magnetic interaction between a lanthanide ion and a second spin carrier, have been performed in the last two decades, as demonstrated by the number of reviews devoted to the magnetic properties of these 3d–4f complexes.^[2–6] Meanwhile, these experimental results have allowed the development of theoretical calculations directed toward a better understanding of the ferromagnetic Cu–Gd interactions.^[7–14] Studies of Co^{II}–Gd complexes have provided an additional and very interesting piece of information.^[15,16] Indeed, ferromagnetic interactions are observed in the complexes presenting high-spin Co^{II} ions and singly occupied 3d_{x²–y²} orbitals ($S=3/2$), whereas these interactions become antiferromagnetic with low-spin Co^{II} ions ($S=1/2$)

having unoccupied 3d_{x²–y²} orbitals. Such an observation confirms the preponderant role played by the 3d_{x²–y²} orbitals, which is in agreement with theoretical results. We have previously published,^[17] along with the group of Matsumoto,^[18] a synthetic pathway yielding tetranuclear [Cu–Gd]₂ complexes. This method is based on a stepwise process involving original mononuclear copper complexes, therefore, we decided to find a route allowing an easy preparation, isolation, and characterization of these key copper complexes. The structural determinations of three mononuclear copper complexes used as ligands in the syntheses of polynuclear Cu–Gd entities confirm the interest of this experimental process. The anionic mononuclear Cu precursors, obtained with ligands possessing three functions that can be deprotonated, yield structurally characterized tetranuclear [Cu–Gd]₂ complexes after reaction with Gd ions and ancillary ligands. The alternate arrangement of the Cu and Gd ions favors Cu–Gd interactions through bridges involving single atom (phenoxo) or three atoms (amidato) bridges and avoids direct Cu–Cu and Gd–Gd interactions. According to the same process, a neutral Cu precursor, in which the Cu ion is surrounded by one phenoxo oxygen atom and three different nitrogen atoms (amide, imine, and pyridine) gives a trinuclear triangular Cu–Gd–Cu complex possessing three atoms amidato Cu–Gd bridges only. Furthermore, we have shown in a recent paper that the Cu–Gd interaction through a single oxime bridge is antiferromagnetic.^[19] A supplementary example is also described in the present paper, thanks to the structural determination of a tetranuclear [Cu–Gd]₂ complex involving a neutral Cu precursor having a unique deprotonated oxime function introducing Cu–Gd interactions through the

[a] Dr. J.-P. Costes, Dr. C. Duhayon, Dr. S. Mallet-Ladeira, Prof. S. Shova, Dr. L. Vendier
Laboratoire de Chimie de Coordination du CNRS
205, route de Narbonne, BP 44099, 31077 Toulouse Cedex 4 (France)
E-mail: jean-pierre.costes@lcc-toulouse.fr

[b] Dr. J.-P. Costes, Dr. C. Duhayon, Dr. S. Mallet-Ladeira, Prof. S. Shova, Dr. L. Vendier
Université de Toulouse; UPS, INPT, 31077 Toulouse Cedex 4 (France)

[c] Prof. S. Shova
Department of Chemistry, Moldova State University
A. Mateevici Str. 60, 2009 Chisinau (Moldova)

Supporting information for this article (containing the crystallographic data in CIF format and the magnetic data) is available on the WWW under <http://dx.doi.org/10.1002/chem.201504238>.

two atoms oximate bridges. These experimental results based on the number of atoms involved in the Cu–Gd bridges, combined to recently published theoretical data, give interesting information on the general M–Gd magnetic interaction.

Experimental Section

Materials: Salicylaldehyde, hexafluoroacetylacetone (Hhfa), 3-(perfluorobutyl)-(-)-camphor (HScamph), 3-(perfluorobutyl)-(+)-camphor (HRcamph), Cu(OAc)₂·2H₂O, and GdCl₃·6H₂O, (Aldrich) were used as purchased. [Gd(hfa)₃]·2H₂O^[20] (hfa = hexafluoroacetylacetonato), [Gd(hfa)₂(Hhfa)(CH₃CO₂)],^[21] and [L¹Cu]^[19] were prepared as previously described. High-grade solvents (diethyl ether, dimethylformamide, acetone, and methanol) were used for the syntheses of ligands and complexes.

Physical measurements: C, H, and N elemental analyses were carried out at the Laboratoire de Chimie de Coordination Microanalytical Laboratory in Toulouse, France. IR spectra were recorded with a Perkin–Elmer Spectrum 100FTIR by using the ATR mode. 1D and 2D ¹H and ¹³C NMR spectra were acquired at 400.16 (500.33) MHz (¹H) or 100.63 MHz (125.82 MHz) (¹³C) on Bruker Avance 400 or 500 spectrometers by using [D₆]DMSO as solvent. Chemical shifts are given in [ppm] versus trimethylsilane (TMS) (¹H and ¹³C). Magnetic data were obtained with a Quantum Design MPMS SQUID susceptometer. Magnetic susceptibility measurements were performed in the temperature range 2–300 K under a 0.1 T applied magnetic field, and diamagnetic corrections were applied by using Pascal's constants.^[22] Isothermal magnetization measurements were performed up to 5 T at 2 K. The magnetic susceptibilities have been computed by exact calculations of the energy levels associated to the spin Hamiltonian through diagonalization of the full matrix with a general program for axial symmetry,^[23] and with the MAGPACK program package^[24] in the case of magnetization. Least-squares fittings were accomplished with an adapted version of the function-minimization program MINUIT.^[25]

Synthesis

Ligands: The syntheses of *N*-(2-amino-2-methylpropyl)-2-hydroxybenzamide,^[17c] 2-hydroxy-*N*-{2-[(1-methylethylidene)amino]ethyl}benzamide,^[17c] and *N*-(2-amino-2-methylpropyl)-2-hydroxy-3-methoxybenzamide^[17b] "half-units" ligands have been previously described.

N-(2-Aminocyclohexyl)-2-hydroxybenzamide (L¹H₂): A mixture of phenyl salicylate (2.14 g, 1 × 10⁻² mol) and 1,2-diaminocyclohexane (1.14 g, 1 × 10⁻² mol) in propane-2-ol (40 mL) was heated to reflux for thirty minutes and then cooled down to room temperature under stirring. The white precipitate, which appeared upon cooling, was filtered off and washed with diethyl ether. Yield: 1.2 g (51%). ¹H NMR (400 MHz, 20 °C, [D₆]DMSO): δ = 1.20–1.30 (m, 4H; CH₂), 1.64–1.68 (m, 2H; CH₂), 1.87–1.90 (m, 2H; CH₂), 2.64–2.69 (m, 1H; CH), 3.63–3.65 (m, 1H; CH), 6.72 (t, *J* = 8 Hz, 1H; C5H), 6.82 (d, *J* = 8 Hz, 1H; C3H), 7.27 (td, *J* = 1.8, 8 Hz, 1H; C4H), 7.86 (dd, *J* = 1.8, 8 Hz, 1H; C6H), 9.39 ppm (l, 1H; NH); ¹³C{¹H} NMR (100.62 MHz, 20 °C, [D₆]DMSO): δ = 24.77 (s, CH₂), 25.09 (s, CH₂), 32.02 (s, CH₂), 33.90 (s, CH₂), 54.83 (s, NHCH), 55.35 (s, NH₂CH), 116.90 (s, ArC1), 117.26 (s, ArC3H), 118.51 (s, ArC5H), 129.08 (s, ArC6H), 133.34 (s, ArC4H), 162.52 (s, ArC2OH), 168.98 ppm (s, OCNH); elemental analysis calcd for C₁₃H₁₈N₂O₂ (234.3): C 66.6, H 7.7, N 12.0; found: C 66.2, H 7.5, N 11.8.

2-Hydroxy-*N*-{2-[(2-hydroxyphenyl)methylene]amino}cyclohexyl}benzamide (L²H₃): A mixture of L¹H₂ (1.20 g, 5.1 × 10⁻³ mol) and salicyl-

aldehyde (0.62 g, 5.1 × 10⁻³ mol) in ethanol (20 mL) was heated to reflux for ten minutes under stirring. The solution was left to stand, overnight, yielding yellow crystals that were filtered off and dried. Yield: 1.1 g (64%). ¹³C{¹H} NMR (100.62 MHz, 20 °C, [D₆]DMSO): δ = 24.37 (s, CH₂), 24.93 (s, CH₂), 31.56 (s, CH₂), 33.81 (s, CH₂), 53.01 (s, NHCH), 70.26 (s, NCH), 115.56 (s, ArC1), 116.85 (s, ArCH), 117.78 (s, ArCH), 118.79 (s, ArCH), 118.89 (s, ArCH), 118.98 (s, ArC1), 127.83 (s, ArCH), 132.62 (s, ArCH), 133.97 (s, ArCH), 134.03 (s, ArCH), 160.57 (s, ArC2OH), 160.86 (s, ArC2OH), 165.48 (s, C=N), 168.96 ppm (s, OCNH); elemental analysis calcd for C₂₀H₂₂N₂O₃ (334.4): C 71.0, H 6.6, N 8.3; found: C 70.7, H 6.4, N 8.2.

L²Cu(C₅H₁₂N) (1): A mixture of L²H₃ (0.34 g, 1 × 10⁻³ mol), Cu(OAc)₂·H₂O (0.20 g, 1 × 10⁻³ mol), and piperidine (0.30 g, 3.5 × 10⁻³ mol) was heated and stirred for one hour. The solution was cooled to room temperature, filtered off and left overnight, giving crystals that were isolated by filtration. Yield: 0.30 g (80%). IR (ATR): $\tilde{\nu}$ = 3301 (w), 2939 (w), 1630 (s), 1611 (s), 1543 (s), 1516 (m), 1446 (m), 1433 (m), 1364 (m), 1314 (s), 1263 (s), 1163 (w), 1031 (w), 907 (m), 756 (w), 756 (w), 707 cm⁻¹ (m); elemental analysis calcd for C₂₅H₃₀CuN₃O₃ (484.1): C 62.0, H 6.3, N 8.7; found: C 61.8, H 6.3, N 8.6.

L²Cu(C₅H₁₂N) (2): A mixture of 2-hydroxy-*N*-{2-[(1-methylethylidene)amino]ethyl}benzamide (0.44 g, 2 × 10⁻³ mol) and salicylaldehyde (0.25 g, 2 × 10⁻³ mol) in methanol (20 mL) was heated to reflux for thirty minutes and then left to cool to room temperature under stirring. Cu(OAc)₂·H₂O (0.40 g, 1 × 10⁻³ mol) and piperidine (0.50 g, 5.9 × 10⁻³ mol) were added. The solution was heated to reflux and stirred for two hours. From the cooled solution, a violet precipitate appeared. It was filtered off and washed with 2-propanol and diethyl ether. Yield: 0.39 g (90%). IR (ATR): $\tilde{\nu}$ = 2923 (w), 2862 (w), 2501 (w), 1632 (s), 1593 (s), 1564 (s), 1519 (s), 1464 (m), 1438 (s), 1391 (s), 1380 (s), 1345 (m), 1311 (m), 1310 (m), 1257 (m), 1194 (w), 1156 (w), 1034 (m), 903 (m), 838 (w), 752 (s), 704 (m), 652 cm⁻¹ (w); elemental analysis calcd for C₂₁H₂₅CuN₃O₃ (431.0): C 58.5, H 5.8, N 9.7; found: C 58.1, H 5.6, N 9.5.

L²Cu(C₅H₁₂N) (3): A mixture of *N*-(2-amino-2-methylpropyl)-2-hydroxybenzamide (0.42 g, 2 × 10⁻³ mol) and salicylaldehyde (0.25 g, 2 × 10⁻³ mol) in methanol (20 mL) was heated to reflux for thirty minutes and then left to cool under stirring. Cu(OAc)₂·H₂O (0.40 g, 1 × 10⁻³ mol) and piperidine (0.50 g, 5.9 × 10⁻³ mol) were added. The solution was heated to reflux and stirred for two hours. From the cooled solution, a violet precipitate appeared. It was filtered off and washed with 2-propanol and diethyl ether. Yield: 0.74 g (80%). IR (ATR): $\tilde{\nu}$ = 2958 (w), 2857 (w), 2580 (w), 2482 (w), 1622 (s), 1594 (s), 1563 (s), 1530 (s), 1466 (m), 1440 (s), 1397 (m), 1386 (s), 1341 (m), 1317 (m), 1310 (m), 1263 (m), 1186 (w), 1147 (w), 1029 (m), 888 (m), 849 (w), 759 (s), 704 (m), 658 cm⁻¹ (w); elemental analysis calcd for C₂₃H₂₉CuN₃O₃ (459.0): C 60.2, H 6.4, N 9.2; found: C 59.8, H 6.3, N 9.0.

[L¹⁰Cu]-MeOH (4): A mixture of *N*-(2-amino-2-methylpropyl)-2-hydroxy-3-methoxybenzamide (0.24 g, 1 × 10⁻³ mol), pyridinecarboxaldehyde (0.11 g, 1 × 10⁻³ mol), Cu(OAc)₂·H₂O (0.20 g, 1 × 10⁻³ mol) and piperidine (0.25 g, 3 × 10⁻³ mol) in methanol (10 mL) was heated to reflux 20 min under stirring and set aside for three days. Crystals were isolated by filtration and washed by acetone and diethyl ether. Yield: 0.20 g (48%). IR (KBr): $\tilde{\nu}$ = 3422 (l), 2950 (w), 2833 (w), 1643 (w), 1598 (s), 1573 (s), 1546 (s), 1464 (m), 1436 (s), 1381 (m), 1369 (s), 1338 (m), 1322 (w), 1261 (m), 1232 (s), 1198 (m), 1149 (w), 1089 (w), 1062 (m), 1023 (w), 956 (w), 856 (m), 820 (w), 774 (m), 739 (s), 679 (w), 630 cm⁻¹ (w); elemental analysis calcd for C₁₉H₂₃CuN₃O₄: C 54.2, H 5.5, N 10.0; found: C 53.9, H 5.3, N 9.8.

[L²Cu(dmfgd)(hfa)₂(dmf)]₂ (5): This complex was obtained by slow crystallization of a solution of [L²Cu](C₅H₁₂N) (0.05 g, 1.0 × 10⁻⁴ mol)

and $[\text{Gd}(\text{hfa})_3] \cdot 2\text{H}_2\text{O}$ (0.08 g, 1.0×10^{-4} mol) in DMF (2 mL). Yield: (0.08 g, 71%). IR (ATR): $\tilde{\nu} = 2936$ (w), 2864 (w), 1648 (s), 1601 (m), 1573 (s), 1530 (s), 1471 (m), 1439 (m), 1396 (m), 1345 (w), 1249 (s), 1207 (s), 1142 (s), 1102 (m), 1074 (w), 955 (w), 919 (w), 844 (w), 797 (m), 764 (m), 740 (m), 658 (m), 638 cm^{-1} (w); elemental analysis calcd for $\text{C}_{72}\text{H}_{70}\text{Cu}_2\text{F}_{24}\text{Gd}_2\text{N}_6\text{O}_{18}$ (2232.9): C 38.7, H 3.2, N 5.0; found: C 38.7, H 3.0, N 4.8.

$[\text{L}^3\text{CuGd}(\text{hfa})_2(\text{dmf})_2]$ (**6**): This complex was obtained by slow crystallization of a solution of $[\text{L}^3\text{Cu}](\text{C}_5\text{H}_{12}\text{N})$ (0.04 g, 1.0×10^{-4} mol) and $[\text{Gd}(\text{hfa})_3] \cdot 2\text{H}_2\text{O}$ (0.08 g, 1.0×10^{-4} mol). In DMF (2 mL) Yield: (0.10 g, 49%); IR (ATR): $\tilde{\nu} = 2939$ (w), 1668 (m), 1648 (s), 1600 (m), 1576 (s), 1555 (m), 1530 (s), 1508 (m), 1475 (m), 1437 (w), 1418 (w), 1405 (m), 1384 (w), 1335 (w), 1258 (s), 1189 (s), 1127 (s), 1107 (m), 1045 (w), 906 (w), 847 (w), 793 (m), 754 (m), 659 (m), 615 cm^{-1} (w). elemental analysis calcd for $\text{C}_{58}\text{H}_{44}\text{Cu}_2\text{F}_{24}\text{Gd}_2\text{N}_6\text{O}_{16}$ (1978.6): C 35.2, H 2.2, N 4.2; found: C 35.0, H 2.1, N 4.0.

$[\text{L}^4\text{CuGd}(\text{Rcamph})_2(\text{CH}_3\text{OH})_2]$ (**7**): To a solution of $[\text{L}^4\text{Cu}](\text{C}_5\text{H}_{12}\text{N})$ (0.15 g, 3.3×10^{-4} mol) in methanol (10 mL) was added $\text{GdCl}_3 \cdot 6\text{H}_2\text{O}$ (0.12 g, 3.3×10^{-4} mol), 3-(perfluorobutyl)-(-)-camphor (0.23 g, 6.5×10^{-4} mol) (RcamphH), and piperidine (0.10 g, 1.2×10^{-3} mol). The mixture was stirred and heated to reflux for 15 min and then cooled to room temperature. The resulting lilac precipitate was filtered off and dried. It was dissolved in diethyl ether and slow diffusion of methanol yielded crystals suitable for XRD analysis. Yield: 0.26 g (60%). IR (ATR): $\tilde{\nu} = 3402$ (l), 2964 (m), 1645 (s), 1600 (s), 1577 (s), 1541 (s), 1520 (m), 1476 (w), 1449 (w), 1414 (m), 1343 (m), 1291 (w), 1225 (s), 1211 (s), 1195 (m), 1177 (s), 1106 (m), 1078 (m), 1039 (w), 931 (w), 891 (m), 812 (w), 760 (m), 748 (m), 705 (w), 628 cm^{-1} (w); elemental analysis calcd for $\text{C}_{104}\text{H}_{122}\text{Cu}_2\text{F}_{28}\text{Gd}_2\text{N}_6\text{O}_{14}$ (2653.7): C 47.1, H 4.6, N 3.2; found: C 46.8, H 4.5, N 3.0.

$[\text{L}^4\text{CuGd}(\text{Scamph})_2(\text{CH}_3\text{OH})_2]$ (**8**): The same experimental process as described for the synthesis of compound **7** but by using 3-(perfluorobutyl)-(-)-camphor (ScamphH) yielded the corresponding complex **8**. Yield: 0.27 g (62%). IR (ATR): $\tilde{\nu} = 3400$ (l), 2962 (m), 1644 (s), 1600 (s), 1577 (s), 1541 (s), 1521 (m), 1476 (w), 1449 (w), 1414 (m), 1342 (m), 1290 (w), 1224 (s), 1211 (s), 1195 (m), 1177 (s), 1106 (m), 1078 (m), 1038 (w), 931 (w), 890 (m), 811 (w), 759 (m), 748 (m), 705 (w), 627 cm^{-1} (w); elemental analysis calcd for $\text{C}_{104}\text{H}_{122}\text{Cu}_2\text{F}_{28}\text{Gd}_2\text{N}_6\text{O}_{14}$ (2653.7): C 47.1, H 4.6, N 3.2; found: C 46.8, H 4.6, N 3.1.

$[\text{L}^5\text{CuGd}(\text{hfa})_2(\text{dmf})_2]$ (**9**): A solution of 2-hydroxy-*N*-[2-[(1-methyl-ethylidene)amino]ethyl]benzamide (0.22 g, 1×10^{-3} mol) and *o*-vanillin (0.15 g, 1×10^{-3} mol) in methanol (15 mL) was heated to reflux and stirred for 20 min. Copper acetate (0.2 g, 1×10^{-3} mol) and piperidine (0.3 g, 3.5×10^{-3} mol) were then added and heating was pursued for 30 min. Then the solution was evaporated and the residue was dissolved in dichloromethane. Evaporation of this solution yielded a pasty product. The copper complex (0.046 g, 1×10^{-4} mol) and $[\text{Gd}(\text{hfa})_3] \cdot 2\text{H}_2\text{O}$ (0.082 g, 1×10^{-4} mol) were mixed in DMF (2 mL). Red crystals appeared a few days later. They were collected by filtration and dried. Yield: 0.045 g (47%). IR (ATR): $\tilde{\nu} = 2944$ (w), 1667 (m), 1649 (s), 1603 (m), 1576 (m), 1541 (m), 1521 (m), 1505 (s), 1472 (m), 1457 (m), 1439 (m), 1402 (m), 1380 (w), 1334 (w), 1295 (m), 1246 (s), 1223 (m), 1193 (s), 1131 (s), 1092 (m), 1059 (m), 984 (w), 949 (w), 900 (w), 851 (w), 791 (m), 766 (w), 747 (m), 739 (m), 709 (w), 683 (w), 658 cm^{-1} (m); elemental analysis calcd for $\text{C}_{66}\text{H}_{62}\text{Cu}_2\text{F}_{24}\text{Gd}_2\text{N}_6\text{O}_{20}$ (2184.8): C 36.3, H 2.9, N 5.1; found: C 36.0, H 2.8, N 4.9.

$[\text{L}^{10}\text{Cu}_2\text{Gd}(\text{hfa})_3](\text{C}_3\text{H}_6\text{O})_3$ (**10**): Addition of $[\text{Gd}(\text{hfa})_3] \cdot 2\text{H}_2\text{O}$ (0.05 g, 6.1×10^{-5} mol) to L^4Cu (0.05 g, 1.2×10^{-4} mol) in acetone (5 mL) gave a solution that was filtered and set aside. Crystals appeared three days later. Yield: 0.05 g (45%). IR (KBr): $\tilde{\nu} = 2974$ (w), 1656 (s), 1580 (s), 1539 (s), 1495 (m), 1449 (m), 1398 (s), 1343 (w), 1254 (s),

1208 (s), 1143 (s), 1099 (w), 1061 (w), 950 (w), 860 (w), 817 (w), 796 (m), 741 (m), 660 (s), 642 cm^{-1} (w); elemental analysis calcd for $\text{C}_{62}\text{H}_{67}\text{Cu}_2\text{F}_{18}\text{GdN}_6\text{O}_{17}$ (1794.6): C 41.5, H 3.8, N 4.7; found: C 41.2, H 3.7, N 4.5.

$[(\text{L}^{11}\text{Cu})_2\text{Gd}_2(\text{CH}_3\text{CO}_2)_2(\text{hfa})_4(\text{H}_2\text{O})]$ (**11**): A mixture of L^{11}Cu (0.07 g, 2.07×10^{-4} mol) and $[\text{Gd}(\text{hfa})_2(\text{Hhfa})(\text{CH}_3\text{CO}_2)]$ (0.17 g, 2.07×10^{-4} mol) in CH_2Cl_2 (10 mL) was heated to reflux for ten minutes and concentrated to half volume. Slow diffusion of pentane yielded crystals suitable for XRD analysis. Yield: 0.04 g (20%). IR (ATR): $\tilde{\nu} = 2975$ (w), 1655 (m), 1633 (m), 1608 (w), 1542 (m), 1525 (m), 1471 (w), 1446 (m), 1396 (w), 1305 (w), 1249 (s), 1188 (s), 1130 (s), 1011 (w), 949 (w), 891 (w), 791 (m), 756 (w), 659 cm^{-1} (m); elemental analysis calcd for $\text{C}_{54}\text{H}_{50}\text{Cu}_2\text{F}_{24}\text{Gd}_2\text{N}_6\text{O}_{17}$: (1952.6) C 33.2, H 2.6 N 4.3; found: C 32.9, H 2.6 N 4.2.

Crystallographic data collection and structure determination for the complexes 1, 2, 3, 4, 5, 10, and 11: Crystals of compounds **1**, **2**, **3**, **4**, **5**, **10**, and **11** were kept in the mother liquor until they were dipped into oil. The chosen crystals were mounted on a Mitegen micromount and quickly cooled down to 180 (compounds **2**, **3**, and **5**), 100 (compound **11**), or 293(2) K (compounds **1**, **4**, and **10**). The selected crystals of compounds **1** (red, $0.625 \times 0.15 \times 0.075 \text{ mm}^3$), **2** (violet, $0.15 \times 0.125 \times 0.05 \text{ mm}^3$), **3** (dark purple, $0.18 \times 0.15 \times 0.04 \text{ mm}^3$), **4** (red, $0.25 \times 0.20 \times 0.15 \text{ mm}^3$), **5** (blue, $0.375 \times 0.25 \times 0.075 \text{ mm}^3$), **10** (red, $0.325 \times 0.15 \times 0.125 \text{ mm}^3$), and **11** (blue, $0.375 \times 0.25 \times 0.075 \text{ mm}^3$) were mounted on a Bruker Kappa Apex II (compounds **2** and **3**), an Oxford Diffraction Gemini (compound **11**), or a Stoe Imaging Plate Diffractometer System (IPDS) (**1**, **4**, **5**, **10**) using molybdenum ($\lambda = 0.71073 \text{ \AA}$) and equipped with an Oxford Cryosystems cooler device. The unit cell determination and data integration were carried out by using XRED,^[26] CrysAlis RED, or SAINT packages.^[27–29] The structures have been solved by using SIR92,^[30] SUPERFLIP,^[31] or SHELXS-97^[32] and they have been refined by least-squares procedures by using the software packages CRYSTALS^[33] or WinGX version 1.63.^[34] Atomic scattering factors were taken from the international tables for X-ray crystallography.^[35] All hydrogen atoms were refined by using a riding model. When it was possible, all non-hydrogen atoms were anisotropically refined. Drawings of the molecules have been performed with the program CAMERON.^[36] CCDC 1055186 (**1**), 1055187 (**2**), 1055188 (**3**), 1055189 (**4**), 1055190 (**5**), 1055191 (**10**), and 1055192 (**11**) contain the supplementary crystallographic data for this paper. These data can be obtained free of charge from The Cambridge Crystallographic Data Centre via www.ccdc.cam.ac.uk/data_request/cif.

Crystal data for compound 1: $\text{C}_{25}\text{H}_{31}\text{CuN}_3\text{O}_3$; $M = 485.07$; monoclinic; $P2_1/c$; $Z = 4$; $a = 11.252(2)$, $b = 19.285(4)$, $c = 11.357(2) \text{ \AA}$; $\alpha = \gamma = 90$, $\beta = 112.66(3)^\circ$; $V = 2274.2(8) \text{ \AA}^3$; 16356 collected reflections; 4458 unique reflections ($R_{\text{int}} = 0.0612$); $R = 0.0393$; $R_w = 0.0538$ for 2759 contributing reflections [$I > 2\sigma(I)$].

Crystal data for compound 2: $\text{C}_{21}\text{H}_{25}\text{CuN}_3\text{O}_3$; $M = 430.98$; orthorhombic; $Pbca$; $Z = 8$; $a = 10.065(5)$, $b = 16.999(5)$, $c = 22.395(5) \text{ \AA}$; $\alpha = \beta = \gamma = 90^\circ$; $V = 3832(2) \text{ \AA}^3$; 14911 collected reflections; 3365 unique reflections ($R_{\text{int}} = 0.0314$); $R = 0.0280$, $R_w = 0.0673$ for 2705 contributing reflections [$I > 2\sigma(I)$].

Crystal data for compound 3: $\text{C}_{23}\text{H}_{29}\text{CuN}_3\text{O}_3$; $M = 459.03$; monoclinic; $P2_1/c$; $Z = 4$; $a = 10.8652(7)$, $b = 15.9059(9)$, $c = 13.0538(8) \text{ \AA}$; $\alpha = \gamma = 90$, $\beta = 109.225(3)^\circ$; $V = 2130.2(2) \text{ \AA}^3$; 34713 collected reflections; 4356 unique reflections ($R_{\text{int}} = 0.0304$); $R = 0.0249$; $R_w = 0.0645$ for 3716 contributing reflections [$I > 2\sigma(I)$].

Crystal data for compound 4: $\text{C}_{19}\text{H}_{23}\text{CuN}_3\text{O}_4$; $M = 420.94$; monoclinic; $P2_1/n$; $Z = 4$; $a = 11.271(2)$, $b = 11.792(2)$, $c = 14.480(3) \text{ \AA}$; $\alpha = \gamma = 90$, $\beta = 110.21(3)^\circ$; $V = 1806.0(6) \text{ \AA}^3$; 12982 collected reflections;

3549 unique reflections ($R_{\text{int}}=0.0617$); $R=0.0378$; $R_w=0.0603$ for 2553 contributing reflections [$I > 2\sigma(I)$].

Crystal data for compound 5: $C_{72}H_{70}Cu_2F_{24}Gd_2N_8O_{18}$; $M=2232.94$; triclinic; $P\bar{1}$; $Z=2$; $a=11.558(5)$, $b=12.101(5)$, $c=18.338(5)$ Å; $\alpha=75.141(5)$, $\beta=87.455(5)$, $\gamma=65.439(5)^\circ$; $V=2249.1(15)$ Å³; 21 836 collected reflections; 8003 unique reflections ($R_{\text{int}}=0.0568$); $R=0.0479$; $R_w=0.1210$ for 6803 contributing reflections [$I > 2\sigma(I)$].

Crystal data for compound 10: $C_{60}H_{59}Cu_2F_{18}GdN_6O_{15}$; $M=1730.5$; orthorhombic; $Pca2_1$; $Z=4$; $a=25.650(5)$, $b=21.370(4)$, $c=12.614(3)$ Å; $\alpha=\beta=\gamma=90.00^\circ$; $V=6914(2)$ Å³; 43 520 collected reflections; 10 948 unique reflections ($R_{\text{int}}=0.1107$); $R=0.0545$; $R_w=0.1070$ for 7304 contributing reflections [$I > 2\sigma(I)$].

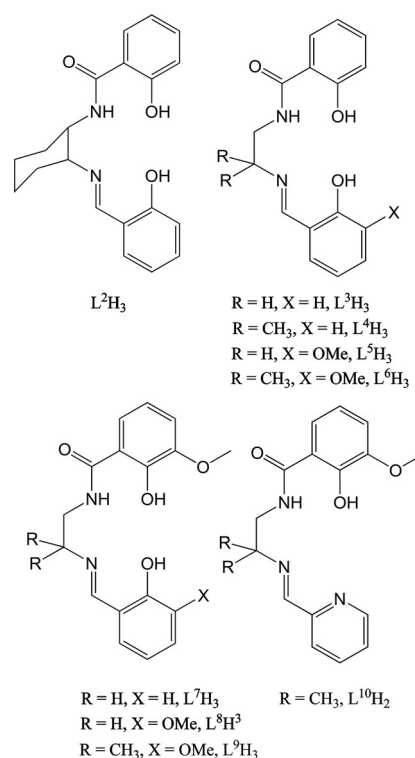
Crystal data for compound 11: $C_{54}H_{50}Cu_2F_{24}Gd_2N_6O_{17}$; $M=1952.58$; monoclinic; $P2_1/n$ (No.14); $Z=4$; $a=18.9557(2)$, $b=18.7083(1)$, $c=20.0267(2)$ Å; $\beta=95.4704(8)^\circ$; $V=7069.7(1)$ Å³; 120 093 collected reflections; 17 445 unique reflections ($R_{\text{int}}=0.037$); $R=0.046$; $R_w=0.051$ for 13 743 contributing reflections [$I > 3\sigma(I)$].

Relevant parameters for complex $[L^4CuGd(Scamph)_2(CH_3OH)_2]$ (7): Space group: $P2_1$; lattice parameters: $a=17.874(5)$, $b=15.377(5)$, $c=20.789(5)$ Å; $\alpha=\gamma=90$, $\beta=112.829(5)^\circ$; $V=5266(3)$ Å³. These data do confirm that complex 8 is tetranuclear with the expected $C_{94}H_{88}Cu_2F_{28}Gd_2N_4O_{16}$ formula and DMF molecules coordinated to the Cu and Gd ions. The non-centrosymmetry comes from the use of a pure enantiomeric (*S*)-camphorate ligand. The cif data are not given due to problems coming from refinement of the fluorinated camphorate chain.

Results and Discussion

Syntheses

The non-symmetric compartmental ligands L^nH_3 with n going from 2 to 9, and $L^{10}H_2$, used in this study have been prepared according to an experimental stepwise procedure,^[17b,c] by reaction of "half-unit" ligands, possessing the amide function, with salicylaldehyde, *o*-vanillin, or pyridinecarboxaldehyde (Scheme 1). Note that we previously reported several "half-unit" ligands, namely, 2-hydroxy-*N*-[2-[(1-methylethylidene)amino]ethyl]benzamide, *N*-(2-amino-2-methylpropyl)-2-hydroxybenzamide,^[17c] and *N*-(2-amino-2-methylpropyl)-2-hydroxy-3-methoxybenzamide^[17b], whereas the preparation of *N*-(2-aminocyclohexyl)-2-hydroxybenzamide has been recently reported.^[37] The L^nH_3 ligands ($n=2$ to 9) possess identical inner N_2O_2 coordination sites with one amide, one imine, and two phenol functions. They slightly differ by their diamino chain but mainly by their outer coordination sites that involve two (O_2), three (O_2O), and four (O_2O_2) oxygen atoms. The ligand $L^{10}H_2$ is made of one amide, one imine, one phenol, and one pyridine functions, the pyridine function replacing a phenol function. The monometallic copper complexes are readily obtained by reaction of the ligands dissolved in methanol with copper(II) acetate in the presence of piperidine as deprotonating agent. The desired $[L^nCu]pipH$ ($pipH$ =piperidine) ($n=2$ to 9) and $L^{10}Cu$ complexes are obtained as crystals from the resulting reaction media with satisfying yields. The complexes 1–3 are ionic whereas complex 4 is neutral, due to the presence of three or only two ligand functions that can be deprotonated. The heterometallic Cu–Gd complexes are isolated by reaction of these precursors with $[Gd(hfa)_3]\cdot 2H_2O$ (hfa =hexafluoro-



Scheme 1. Schematic representation of the various ligands used within this study. L^2H_3 = 2-hydroxy-*N*-(2-[(2-hydroxyphenyl)methylene]amino)cyclohexyl)benzamide, L^3H_3 = 2-hydroxy-*N*-(2-[(2-hydroxyphenyl)methylene]amino)ethyl)benzamide, L^4H_3 = 2-hydroxy-*N*-(2-[(2-hydroxyphenyl)methylene]amino)-2-methylpropyl)benzamide, L^5H_3 = 2-hydroxy-*N*-(2-[(2-hydroxy-3-methoxyphenyl)methylene]amino)ethyl)benzamide, L^6H_3 = 2-hydroxy-*N*-(2-[(2-hydroxyphenyl)methylene]amino)-2-methylpropyl)benzamide, L^7H_3 = 2-hydroxy-*N*-(2-[(2-hydroxyphenyl)methylene]amino)ethyl)-3-methoxybenzamide, L^8H_3 = 2-hydroxy-*N*-(2-[(2-hydroxyphenyl)methylene]amino)-2-methylpropyl)-3-methoxybenzamide, L^9H_3 = 2-hydroxy-*N*-(2-[(2-hydroxy-3-methoxyphenyl)methylene]amino)-2-methylpropyl)-3-methoxybenzamide, $L^{10}H_2$ = 2-hydroxy-3-methoxy-*N*-(2-methyl-2-[(pyridine-2-ylmethylidene)amino]propyl)benzamide.

acetylacetonato ligand) or $GdCl_3\cdot 6H_2O$ and the 3-(perfluorobutyl)-camphor ligands (i.e., *ScamphH* or *RcamphH*) in methanol. According to chemical analysis, they are well represented by the formulae $[L^nCuGd(X)_2]$ ($L^n=L^2$ to L^9 trianionic ligands) with or without DMF or methanol molecules (X =nitrate, *hfa*, or camph anion). Due to the dianionic nature of the $L^{10}H_2$ ligand, the analytical results confirm a 2:1 Cu/Gd ratio and the formulation $[(L^{10}Cu)_2Gd(hfa)_3]$, with replacement of the two water molecules present in $[Gd(hfa)_3]\cdot 2H_2O$ by two $L^{10}Cu$ fragments. On the contrary the $L^{11}Cu$ copper complex with a unique oxime function is known to react with $[Gd(hfa)_3]\cdot 2H_2O$ to give a dinuclear $[L^{11}CuGd(hfa)_3(H_2O)]$ entity that was characterized by analytical results and magnetic properties.^[19b] The structural determination of the complex resulting from reaction of $[L^{11}Cu]$ with $[Gd(hfa)_2(Hhfa)(CH_3CO_2)]$ indicates that we are dealing with a tetranuclear complex giving a new example of oximate Cu–N–O–Gd bridges.

Description of the structures

The asymmetric units of complexes **1**, **2**, and **3** comprise the monoanionic entities L^2Cu , L^3Cu , or L^4Cu with their cationic piperidinium counterparts (Figure 1 for complex **1** and Figures S1 and S2 in the Supporting Information for complexes **2** and **3**, respectively). They crystallize in the monoclinic space

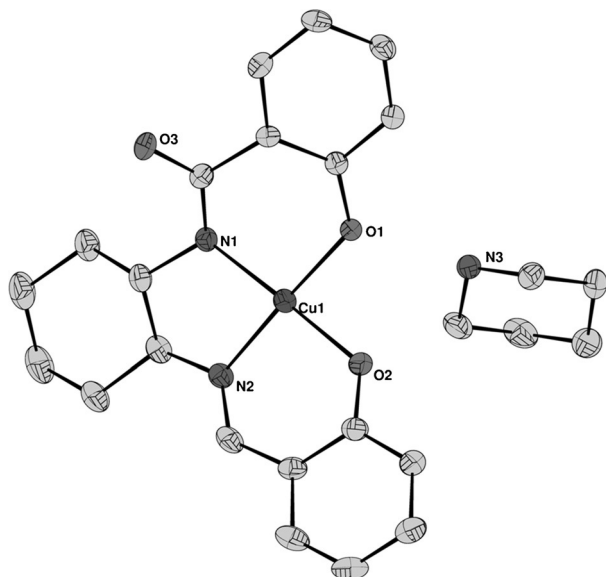


Figure 1. View of the mononuclear complex $[L^2Cu(C_5H_{12}N)]$ (**1**).

groups $P2_1/c$ (complexes **1** and **3**) or $Pbca$ (complex **2**). The Cu^{II} ions are in the trianionic N_2O_2 coordination sites, linked in a square-planar environment to the amidato and imine nitrogen atoms and the two phenoxo oxygen atoms, with similar Cu–O and Cu–N bond lengths for complexes **1**, **2** and **3** (see Table 1), the amide oxygen atom being not involved in the coordination. There are hydrogen bonds involving the free amide oxygen atom, the piperidinium cation, and the phenoxo oxygen atom located on the phenyl cycle bearing the amide

function in the two complexes **1** and **2**, thus giving 1D chains. The alternate arrangement of (R,R) - L^2Cu and (S,S) - L^2Cu units in complex **1** yields a racemate chain. The head-to-tail arrangement of two L^4Cu units yields a hydrogen-bonded dinuclear entity in complex **3**.

Replacement of a phenol function by a pyridine nitrogen atom in complex **4** gives a neutral $[L^{10}Cu]$ species (Figure S3 in the Supporting Information) with the Cu^{II} ion in the dianionic N_3O coordination site. The copper ion remains in a square-planar environment but the presence of cycles involving 6-5-5 atoms around the Cu ion instead of a 6-5-6 surroundings in complexes **1**–**3** shortens the Cu–O and Cu–N(amide) bonds.

Crystals were obtained for complexes **5** and **7**. Due to their similarity, we only describe in detail complex **5**. In these complexes two heteronuclear Cu–Gd entities are assembled in a head-to-tail arrangement through the oxygen atoms of the amidato groups to form a double (Cu–N–C–O–Gd) bridge leading to a tetranuclear entity (Figure 2). In the dinuclear Cu–Gd

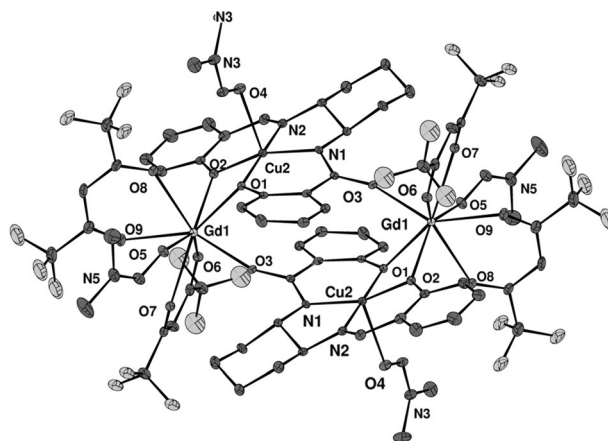
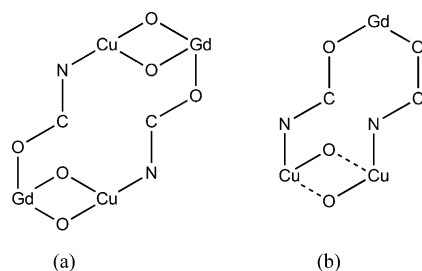


Figure 2. View of the tetranuclear complex **5**. Selected bond lengths [Å] and angles [°]: Cu2–N2 1.934(5), Cu2–N1 1.951(4), Cu2–O1 1.914(4), Cu2–O2 1.977(4), Cu2–O4 2.388(4), O3–C23 1.290(7), Gd1–O2 2.373(4), Gd1–O1 2.411(4), Gd1–O3 2.252(4), Gd1–O5 2.374(4), Gd1–O6 2.390(4), Gd1–O7 2.469(4), Gd1–O8 2.480(4), Gd1–O9 2.450(4) Å; Gd1–O1–Cu2 102.7(1), Gd1–O2–Cu2 102.1(1)°.

Table 1. Selected bond lengths and angles for the mononuclear copper complexes **1**–**4**.

	$[L^2Cu(C_5H_{12}N)]$ (1)	$[L^3Cu(C_5H_{12}N)]$ (2)	$[L^4Cu(C_5H_{12}N)]$ (3)	$[L^{10}Cu]$ (4)
bond lengths [Å]				
Cu1–N1	1.932(2)	1.912(2)	1.914(1)	1.883(2)
Cu1–N2	1.923(2)	1.936(2)	1.950(1)	1.952(2)
Cu1–O1	1.877(2)	1.902(2)	1.907(1)	1.862(2)
Cu1–O2	1.913(2)	1.911(2)	1.908(1)	
Cu1–N3				1.995(2)
O–C amide	1.260(3)	1.266(3)	1.263(2)	1.254(3)
angles [°]				
O1–Cu1–O2	86.06(7)	86.50(6)	87.47(5)	
O1–Cu1–N1	95.56(8)	94.86(7)	94.35(5)	98.16(9)
N2–Cu1–N1	86.31(9)	86.05(8)	85.41(6)	84.88(9)
O2–Cu1–N2	92.11(8)	92.79(7)	93.53(5)	
O1–Cu1–N3				97.52(9)
N2–Cu1–N3				81.09(9)

units, the two ions are doubly bridged by two phenoxo oxygen atoms belonging to the L^2 ligand with Cu...Gd separations of 3.393(1) Å. The bridging network is reported in Scheme 2a. The copper ion is penta-coordinate, with a long axial Cu–O(dmef) bond length (i.e., 2.388(2) Å). The gadolinium ions are eight-coordinate, surrounded by five supplementary oxygen atoms coming from two ancillary hfa molecules and one DMF molecule. The bridging networks Cu–(O₂)–Gd are not planar, with hinge angles between the (O–Cu–O) and (O–Gd–O) planes equal to 20.8(1)°. The intermolecular copper–copper separations are shorter (i.e., 8.516(2) Å) than the Gd...Gd distances (i.e., 10.891(2) Å). They preclude any significant interaction of magnetic nature between these tetranuclear units.



Scheme 2. Bridging motive in a) complexes 5 and 7 and b) complex 10.

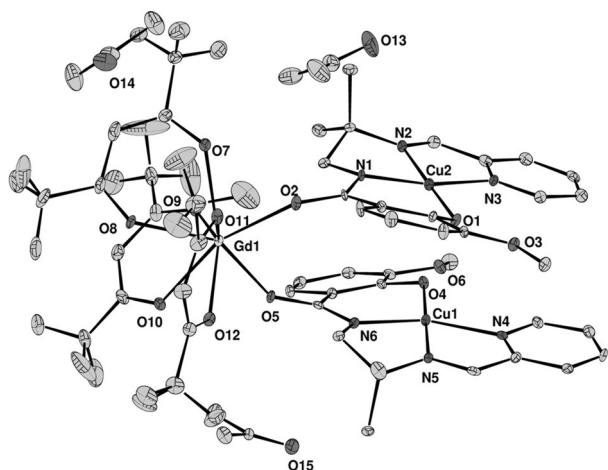


Figure 3. View of the trinuclear complex 10. Selected bond lengths [Å] and angles [°]: Cu1–N4 2.018(8), Cu1–N5 1.932(8), Cu1–N6 1.890(8), Cu1–O4 1.875(7), Cu2–O1 1.880(6), Cu2–N1 1.971(9), Cu2–N2 1.957(8), Cu2–N3 1.889(7), O2–C11 1.289(11), O5–C29 1.324(12), Gd1–O2 2.258(8), Gd1–O5 2.280(7), Gd1–O7 2.425(9), Gd1–O8 2.400(5), Gd1–O9 2.409(7), Gd1–O10 2.467(7), Gd1–O11 2.437(8), Gd1–O12 2.373(7) Å; Cu1–O1–Cu2 94.71(3), Cu1–O4–Cu2 98.02(4)°.

The asymmetric unit of complex 10 consists of the trinuclear neutral $[(L^{10}Cu)_2Gd(hfa)_3]$ unit, shown in Figure 3, and three acetone molecules crystallizing in the orthorhombic space group $Pca2_1$. Two $L^{10}Cu$ molecules are linked to a gadolinium ion through their oxygen amide atom (2.258(8) and 2.280(7) Å for Gd–O2 and Gd–O5, respectively) and the three ions are located at the apexes of a practically perfect isosceles triangle (Gd...Cu1 = 5.837(2), Gd...Cu2 = 5.897(2) Å, with Cu1...Cu2 = 3.457(2) Å). The copper ions are five-coordinate, linked to the N_3O inner coordination site of the dideprotonated L^{10} ligand, the fifth axial coordination coming from the phenoxo function of the neighboring $L^{10}Cu$ unit (Cu1–O1 = 2.751(1) and Cu2–O4 = 2.655(1) Å and Cu–O–Cu angles of 94.7(1) and 98.0(1)°, respectively), thus inducing a triangular arrangement of the present trinuclear complex (see Scheme 2b). The gadolinium ions are again eight-coordinate to the six oxygen atoms belonging to three hfa ligands and to two oxygen amide atoms coming from the two $L^{10}Cu$ units.

Complex 11 is a tetranuclear complex made of two $L^{11}Cu$ units linked to two different Gd ions by the oxygen atoms of their oxime functions, as shown in Figure 4. A schematic representation of the metal ions interaction pathways with the numbering of the oxygen atoms retained in the structure is

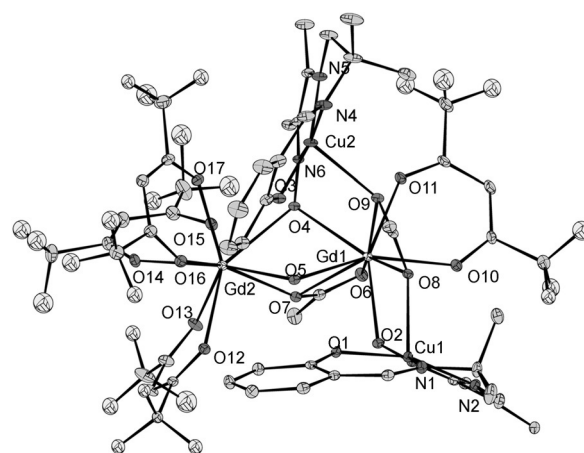
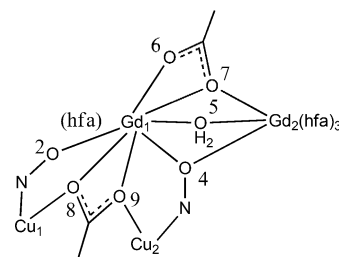


Figure 4. View of the tetranuclear $[Cu-Gd]_2$ complex 11. Selected bond lengths [Å] and angles [°]: Cu1–N1 1.963(4), Cu1–N2 1.946(4), Cu1–N3 1.993(4), Cu1–O1 1.926(3), Cu1–O8 2.289(3), Cu2–N4 1.953(4), Cu2–N5 1.959(4), Cu2–N6 1.997(4), Cu2–O3 1.917(3), Cu2–O9 2.327(3), Gd1–O2 2.318(3), Gd1–O4 2.382(3), Gd1–O5 2.584(3), Gd1–O6 2.453(4), Gd1–O7 2.499(3), Gd1–O8 2.489(3), Gd1–O9 2.486(3), Gd1–O10 2.406(3), Gd1–O11 2.439(3), Gd2–O4 2.479(3), Gd2–O5 2.569(3), Gd2–O7 2.390(3), Gd2–O12 2.435(3), Gd2–O13 2.469(4), Gd2–O14 2.357(3), Gd2–O15 2.400(3), Gd2–O16 2.424(3), Gd2–O17 2.409(4), Gd1...Gd2 3.8678(3) Å; Cu1–N3–O2 123.8(3), Cu2–N6–O4 126.6(3), Cu1–O8–C33 136.3(3), Cu2–O9–C33 128.1(3), Gd1–O2–N3 117.4(2), Gd2–O4–N6 128.5(2), Gd1–O5–Gd2 97.3(1), Gd1–O7–Gd2 104.6(1), Gd1–O4–Gd2 105.4(1)°.



Scheme 3. Bridging motive in complex 11.

given in Scheme 3. The copper ions are bridged together by an acetate group occupying the axial position of each copper ion and linking the two copper ions in an *anti-anti* coordination mode with a Cu...Cu distance of 6.278(4) Å whereas it chelates at the same time a Gd ion in a *syn-syn* mode. The two Gd ions are linked by three different bridges, a supplementary μ -acetato-1,2- κ -O_i-2- κ -O', a μ -oximato-1,2- κ -O, and a water molecule bridged in a μ -1,2- κ -O mode, according to the kappa convention. The two Gd ions are nona-coordinate. The Gd2 ion is linked to the three oxygen atoms of the bridges and to six oxygen atoms coming from three chelating hexafluoroacetylacetonato ligands whereas the Gd1 ion is coordinated to an acetate ligand and to a chelating hexafluoroacetylacetonato ligand, linked to an oximato oxygen atom and to four oxygen atoms from the three bridges. The single oximato Gd1–O2 bond (2.318(3) Å) is shorter than the oximato-bridged one (2.382(3) Å for Gd1–O4 and 2.479(3) Å for Gd2–O4). The Gd1 ion is chelated by the two acetate ligands with bonds varying from 2.453(4) to 2.499(3) Å but the η^2 oxygen atom of the bridging acetate group presents two different bond lengths

(2.390(3) Å for Gd2–O7 vs. 2.499(3) Å for Gd1–O7). The water molecule is located in a practically symmetrical position in between the two Gd ions (2.584(3) vs. 2.569(3) Å). This results in a Gd...Gd distance of 3.868(3) Å. Although the Cu1...Gd1 and Cu2...Gd1 distances are equivalent, that is, 4.030(3) and 4.054(3) Å, the Cu2...Gd2 distance is larger (4.636(4) Å).

Magnetic properties

The magnetic susceptibility of the tetranuclear Cu₂–Gd₂ complexes **5**, **6**, **7**, **8**, and **9** have been measured in the temperature range 2–300 K in a 0.1 T applied magnetic field. As an example the thermal variation of the $\chi_M T$ versus T plot of complex **5** is shown in Figure 5, with χ_M being the molar magnetic susceptibility of the tetranuclear complex, corrected for the diamagnetism of the ligands.^[22] At 300 K, the $\chi_M T$ value is equal to 16.53 cm³ mol⁻¹ K, which is in agreement with the expected value for two Cu^{II} ions and two Gd^{III} ions, which are uncoupled (i.e., 16.50 cm³ mol⁻¹ K with $g=2$). Lowering the temperature causes the $\chi_M T$ value to increase and reach a value of 29.34 cm³ mol⁻¹ K at 2 K, which is larger than expected (2 × 10 cm³ mol⁻¹ K) for two uncorrelat-

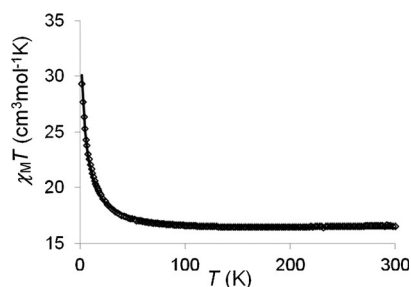


Figure 5. Temperature dependence of the product $\chi_M T$ for complex **5** at a 0.1 T applied magnetic field. The solid line corresponds to the best data fit (see text).

ed pairs of ferromagnetically coupled Cu^{II} and Gd^{III} ions but smaller than the maximum value (36 cm³ mol⁻¹ K), which is attributable to a $S=8$ spin state resulting from the ferromagnetic coupling of two Cu–Gd pairs. Such a behavior is consistent with the simultaneous occurrence of two ferromagnetic Cu–Gd interactions, which operate within each Cu–Gd pair and between two pairs, respectively. A quantitative analysis based on a “dimer of dimer” model directly derived from the structural data and by using the Hamiltonian $H = -J(S_{Cu}S_{Gd} + S_{Cu'}S_{Gd'}) - J'(S_{Cu}S_{Cu'} + S_{Gd}S_{Gd'}) + \sum_{ij} g_i g_j \beta H_i S_{ij}$ with the terms gauged by the J and J' parameters accounting for the spin exchange and the last term accounting for the Zeeman contributions where $i=Cu$ and Gd , and $j=x, y$, and z , leads to $J=4.17(5)$ cm⁻¹, $J'=0.77(5)$ cm⁻¹, and $g=1.99$ with an agreement factor R ($R = \frac{\sum[(\chi T)_{obs} - (\chi T)_{calc}]^2}{\sum[(\chi T)_{obs}]^2}$) equal to 7×10^{-5} . The two coupling constants characterizing complex **5** differ by an order of magnitude so that their respective pathways are easily recognized, the larger value corresponding to the

double phenoxo Cu(O₂)–Gd bridged form and the lower value to the single amidato bridge (Cu–N–C–O–Gd'), which is in agreement with previous results.^[17,18] The magnetic studies of the other [Cu–Gd]₂ complexes (i.e., complexes **6**–**9**) give similar data, which are reported in Table 2, the thermal variations of the $\chi_M T$ versus T plots appearing in the Supporting Information (Figures S4–S7). Table 2 also reports the magnetic data coming from previously published tetranuclear complexes.^[17,18] Confir-

Table 2. Interaction parameters found in tetranuclear [Cu–Gd]₂ complexes possessing alternate double phenoxo and amidato bridges.

Complex	J [cm ⁻¹]	J' [cm ⁻¹]	g	R	Reference
[L ² CudmfGd(hfa) ₂ dmf] ₂	4.17	0.77	1.98	7×10^{-5}	compound 5
[L ³ CuGd(hfa) ₂ dmf] ₂	1.95	0.46	1.99	4.6×10^{-5}	compound 6
[L ⁴ CuGd(hfa) ₂ MeOH] ₂	3.20	0.54	2.00	3×10^{-5}	[17a]
[L ⁴ CudmfGd(camph+) ₂ dmf] ₂	2.44	0.61	2.00	6×10^{-5}	compound 7
[L ⁴ CudmfGd(camph-) ₂ dmf] ₂	2.87	0.51	2.04	1.5×10^{-5}	compound 8
[L ⁵ CuGd(hfa) ₂ dmf] ₂	3.85	0.53	2.04	1.1×10^{-5}	compound 9
[L ⁵ CuGd(hfa) ₂ MeOH] ₂	6.2	2.4	2.02	2×10^{-5}	[18a]
[L ⁶ CuGd(NO ₃) ₂ OH] ₂	5.89	0.82	1.99	4×10^{-5}	[17b]
[L ⁷ CuGd(NO ₃) ₂ OH] ₂	2.80	0.64	1.99	1×10^{-4}	[17b]
[L ⁸ CuGd(NO ₃) ₂ MeOH] ₂	7.96	0.82	1.99	1×10^{-5}	[17b]
[L ⁹ CuGd(NO ₃) ₂ MeOH] ₂	6.94	0.58	1.99	1×10^{-5}	[17d]

mation of the nature of the ground state and, consequently of the nuclearity of complex **8** is afforded by the field dependence of the magnetization M at 2 K (Figure S8 in the Supporting Information). Increasing the field up to 5 T causes the magnetization to approach the saturation value of 16 N β units, which is consistent with a $S=8$ and $g=2$ system.

The thermal variation of the $\chi_M T$ versus T plot for the trinuclear complex **10** goes from 8.5 cm³ mol⁻¹ K at 300 K to 9.11 cm³ mol⁻¹ K at 2 K. As this variation is weak, Figure 6 only reports the data from 100 to 2 K. In that case the experimental data can be properly fitted by using an Hamiltonian, taking into account Cu–Gd and Cu–Cu interactions, that is, $H = -J(S_{Cu}S_{Gd} + S_{Cu'}S_{Gd'}) - J'(S_{Cu}S_{Cu'}) + \sum_{ij} g_i g_j \beta H_i S_{ij}$, which yields $J=0.40(2)$ cm⁻¹, $J'=-2.60(5)$ cm⁻¹, $g=1.99$, and $R=7.5 \times 10^{-4}$. These values allow to fit the field dependence of the magnetization M at 2 K (Figure S9 in the Supporting Information), with a saturation value at 5 T equal to 8.7 N β corresponding to an $S=9/2$ and $g=2$ ground state. The magnetization curve does

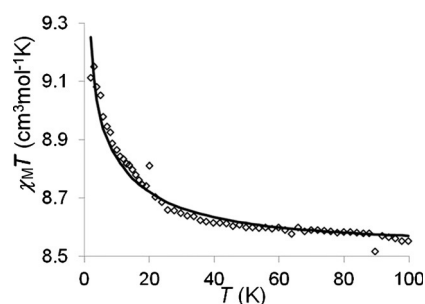


Figure 6. Temperature dependence of the product $\chi_M T$ for complex **10** at a 0.1 T applied magnetic field. The solid line corresponds to the best data fit (see text).

not present a sigmoidal form because the $J(\text{Cu,Gd})$ interaction is ferromagnetic, with a value which is in complete agreement with those obtained in the tetranuclear species.

In the tetranuclear complex **11**, the product $\chi_M T$ remains practically constant and equal to $16.15 \text{ cm}^3 \text{ mol}^{-1} \text{ K}$ from 300 to 50 K, where it begins to decrease till a value of $13.49 \text{ cm}^3 \text{ mol}^{-1} \text{ K}$ at 2 K (Figure 7). A value of $16.5 \text{ cm}^3 \text{ mol}^{-1} \text{ K}$ is expected at room temperature for two Cu and two Gd ions, which do not interact. In view of the structural determination, we have to take into account at least two different Cu–Gd interactions along with a Gd–Gd interaction. Nevertheless, we

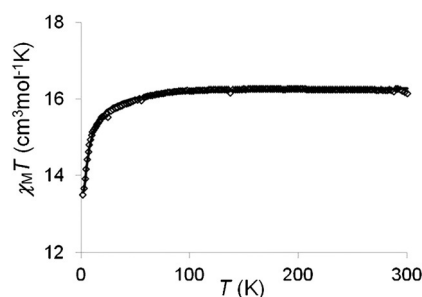


Figure 7. Temperature dependence of the product $\chi_M T$ for complex **11** at a 0.1 T applied magnetic field. The solid line corresponds to the best data fit (see text).

can eliminate the Cu–Cu interaction, because the *anti-anti* acetate bridge links the two Cu ions in their axial position, where the spin density is expected to be almost zero. Concerning the Gd–Gd interaction, the μ -acetato-1,2- κ -O,-2- κ -O' bridge is known to induce ferromagnetic interactions,^[38–40] whereas the bridging oxygen atoms of water molecules and oxime functions^[41] are expected to yield antiferromagnetic interactions. As these interactions are always weak, these antagonist effects should give a very weak parameter. We have previously shown that the Cu–Gd interaction through an oxime bridge is antiferromagnetic.^[19] The best fit obtained with the Hamiltonian $H = -J_1(S_{\text{Cu}1}S_{\text{Gd}1}) - J_2(S_{\text{Cu}2}S_{\text{Gd}1} + S_{\text{Cu}2}S_{\text{Gd}2}) - J_3(S_{\text{Gd}1}S_{\text{Gd}2}) + \sum_{ij} g_i g_j \beta^2 H_i S_{ij}$, which yields $J_1(\text{Cu,Gd}) = -0.36(5) \text{ cm}^{-1}$, $J_2(\text{Cu,Gd}) = -0.19(5) \text{ cm}^{-1}$, $J_3(\text{Gd,Gd}) = -0.023(5) \text{ cm}^{-1}$, $g = 1.99$, and $R = 1 \times 10^{-5}$, which is in complete agreement with our expectation. Due to the presence of several interaction parameters, this result is subject to caution, concerning the type of the very weak Gd–Gd interaction but this supplementary example confirms that the Cu–Gd interaction through the oxime bridge is antiferromagnetic, which is in agreement with our previous results.^[19]

Discussion

These results clearly demonstrate that the use of ligands possessing amide, imine, and phenoxo functions yield tetranuclear $[\text{Cu-Gd}]_2$ complexes with an alternate arrangement of the Cu and Gd ions linked by bridges involving one oxygen atom (phenoxo bridge) or three atoms (O–C–N) for the interaction through the amide bridge. Whatever the nature of the outer coordination site is, O_2 for the ligands L^2 , L^3 , and L^4 , O_3 for the ligands L^5 , L^6 , and L^7 , O_4 for the ligands L^8 and L^9 , tetranuclear complexes are isolated if an ancillary ligand (namely, hfa or

camph) able to chelate the Gd ion is added to the reaction medium. With nitrate anions, ligands having O_4 and O_3 outer coordination sites are needed to obtain tetranuclear complexes. The solvent (MeOH or DMF) completes the Gd coordination sphere, yielding eight-coordinate Gd ions with the ligands L^2 – L^4 and nine-coordinate Gd ions with the ligands L^5 – L^7 . Note that the Gd ions remain nine-coordinate in the case of ligands L^8 and L^9 with their O_4 outer coordination sites, due to the absence of coordinated solvent. Methanol never enters the Cu coordination sphere whereas DMF can coordinate in the axial position with ligands presenting methyl groups on their diamino chain (i.e., ligands L^2 , L^4 , and L^6). Two Cu–Gd interaction pathways are present in these complexes, one through a double phenoxo bridge and the other one through the amidato bridge. The magnetic studies demonstrate that ferromagnetic Cu–Gd interactions are active in the two cases, with J values varying from 2 to 10 cm^{-1} for the double phenoxo bridge and from 0.4 to 1.1 cm^{-1} for the amidato bridge (J' parameter).^[17,18] A view at Table 2 indicates that the larger J values involve complexes possessing nitrate ligands in the Gd coordination sphere. The organic hfa and camph ligands, which imply larger steric constraints, yield lower J values. On the contrary, it is difficult to find a correlation for the J' parameter, as for example the change from nine-coordinate to eight-coordinate of the gadolinium coordination spheres.

We tried to simplify the magnetic analysis with the design of the new L^{10}H_2 ligand in which pyridine replaces one phenol function. Two possible gadolinium coordination modes to the neutral copper complex were expected, that is, through the single phenoxo oxygen atom or through the oxygen atom of the amide function. The structural determination of complex **10** confirms a coordination through the amide bridge, but the triangular arrangement of this complex introduces a slight antiferromagnetic Cu–Cu interaction favored by the weak axial coordination of each Cu ion to the phenoxo oxygen atom of the neighboring L^{10}Cu unit, thus yielding a double phenoxo bridge (Scheme 2b) with long Cu1–O1 (2.751(1) Å) and Cu2–4 (2.655(1) Å) bond lengths. The magnetization curve at 2 K tends to the expected value for an $S=9/2$ ground state without showing a sigmoidal form (Figure S9 in the Supporting Information). With help of that complex it becomes clear that the Cu–Gd interactions through the three atoms amidato bridge are comprised in the range 0.4 – 1 cm^{-1} .

We have recently shown that the Cu–Gd interaction through the oximato bridge made of an even number of atoms, that is, nitrogen and oxygen atoms, is surprisingly antiferromagnetic in complexes formulated as $[(\text{L}^{11}\text{Cu})_2\text{Gd}(\text{NO}_3)_3(\text{H}_2\text{O})]$ and $[\text{L}^{11}\text{CuGd}(\text{hfa})_3]$.^[19] The use of $[\text{Gd}(\text{hfa})_2(\text{Hhfa})(\text{CH}_3\text{CO}_2)]$ as starting material instead of $[\text{Gd}(\text{hfa})_3] \cdot 2\text{H}_2\text{O}$ allowed the isolation and structural determination of a tetranuclear complex. Unfortunately, the presence of different Cu–Gd interactions along with Gd–Gd interaction pathways does not simplify the magnetic study. Nevertheless, this complex does confirm the antiferromagnetic character of the Cu–Gd interaction through the oximato bridge.

Previous and present results indicate that the $3d_{x^2-y^2}$ orbitals play an important role in the Cu–Gd magnetic interaction.

Indeed the Cu–Gd complexes with double phenoxo bridges (edge-sharing complexes) give the largest ferromagnetic interactions. In these complexes, the main structural parameter is the M–(O₂)–Gd hinge angle, defined as the angle between the O–M–O and O–Gd–O planes of the bridging unit. A hinge angle of 1.7(2)° is associated with a *J* coupling constant of 10.1 cm⁻¹,^[42] whereas a hinge angle of 41.6(2)° gives a *J* value of 0.2 cm⁻¹.^[43] Similar examples are found in Ni–Gd complexes.^[44,45] Furthermore, a powerful example is also given by the Co–Gd complexes in which Co^{II} ions are in a high-spin state and penta-coordinate or in a low-spin state and square-planar coordinate.^[15] So the complex [L³CoGd(thd)₂(MeOH)]₂ (thd = tetramethylheptanedionato), in which the Co ion is in a low-spin state, presents an antiferromagnetic interaction (*J*(Co,Gd) = -0.9 cm⁻¹) through the double phenoxo bridge.^[15b] And the complex [L⁵Co(MeOH)Gd(thd)(MeCOO)]₂, with its penta-coordinate and high-spin state Co ion, gives ferromagnetic interactions through the double phenoxo (*J*(Co,Gd) = 0.40 cm⁻¹) and amidato (*J'*(Co,Gd) = 0.24 cm⁻¹) bridges.^[15a] In the low-spin case the 3d_{x²-y²} cobalt orbitals are unoccupied and the Co–Gd interaction is antiferromagnetic,^[15b] whereas the Co–Gd interaction becomes ferromagnetic in the high-spin case with a single occupation of the 3d_{x²-y²} orbital.^[15a,16] Moreover, the entire set of dinuclear M–Gd complexes in which the M ions do possess singly occupied d_{x²-y²} orbitals (M = Cu^{II},^[42] Ni^{II},^[44,45] Co^{II}(high-spin state),^[15,16,46] Fe^{II}(high-spin state),^[46,47] or Mn^{II}(high-spin state)^[46,48,49] do present ferromagnetic interactions through the double phenoxo bridge. On the contrary, weak antiferromagnetic interactions through the double phenoxo bridge are observed in Co^{II}(low-spin state)–Gd,^[15a] Cr^{III}–Gd,^[50,51] and Mn^{III}–Gd compounds,^[52,53] with unoccupied 3d_{x²-y²} orbitals. These results have a double interest. As they highlight the role of the d_{x²-y²} orbital of the 3d ions, they give a direct confirmation for the participation of the 5d Gd orbitals to the interaction mechanism. Some 5d orbitals of Gd being of the same symmetry as the 3d_{x²-y²} molecular orbital of the transition-metal atom, delocalization may take place between them, which will result in the appearance of some spin density in these Gd orbitals. This small delocalization tail of the magnetic orbital centered on the transition-metal atom will induce a magnetic coupling with the unpaired electrons of the Gd atom. Furthermore the angular dependence of the *J* parameter eliminates the participation of the spherical 6s orbital.

Till now, there appeared several theoretical papers devoted to the understanding of the Cu–Gd interaction.^[7–14] We must keep in mind that in the case of Ln ions, the 4f orbitals are shielded and that the 6s and 5d orbitals are the outer orbitals. Although the 5d Gd orbitals are expected to be empty, it has been shown that these 5d orbitals must be included in the calculations to reproduce the experimental *J* values.^[7,9,10,14] So Ruiz et al. demonstrated that the 5d Gd orbitals have a positive spin population, which has to be taken into account to calculate the *J* parameters, and that the 5d spin population does neither come from a 5d–4f mixing nor from a spin transfer of the 3d orbitals.^[14] Their conclusion indicates that the spin polarization of the metal–ligand bonding electron pairs involving the formally empty 5d orbitals is the predominant mechanism.

Whether the appearance of a spin density in the 5d orbitals results from a spin delocalization of monoelectronic origin, or from a spin polarization phenomenon of bi-electronic nature, is not clear. This question would require some restricted versus unrestricted calculations.^[54] For convenience, and as frequently done, we use hereafter the term spin polarization for the introduction of spin densities from remote unpaired electrons.

The results reported in this paper furnish an experimental support playing again in favor of an active spin polarization in 3d Gd complexes. Indeed we show that oxygen phenoxo bridges (single atom bridges) and deprotonated O–C–N amide bridges (three-atom bridges) transmit ferromagnetic interaction when the oximato bridge (two-atom bridge) transmits antiferromagnetic interaction. When spin polarization is active an odd number of bridging atoms in between the ions bearing the spins favors a parallel alignment of the spins, whereas an even number of bridging atoms favors an antiparallel alignment.^[55–57] So this could explain why the oxime function, with its nitrogen and oxygen atoms in between the Cu and Gd ions, is responsible for the presence of an antiferromagnetic Cu–Gd interaction when the phenoxo function with its unique oxygen atom and the amide bridge with three oxygen, carbon and nitrogen atoms give a ferromagnetic Cu–Gd interaction. As spin polarization is transmitted through bonds,^[55] we can understand that the complexes with planar M–O₂–Gd cores favor a better interaction between the σ 3d_{x²-y²} orbitals and the weakly populated 5d Gd orbitals.^[42,45]

Conclusions

This paper reports on a straightforward process for easy preparation and isolation of genuine mononuclear copper complexes, accomplished by the use of piperidinium counterions. In these complexes the copper ions are chelated in a N₂O₂ coordination site by ligands with three functions that can be deprotonated and a supplementary oxygen atom that belongs to an amide function, which, at a later stage, is able to coordinate to Gd ions to yield heterotetranuclear [Cu–Gd]₂ complexes. The resulting [Cu–Gd]₂ complexes, in which the Cu and Gd ions are alternately arranged, clearly shows that Cu–Gd interactions through bridges made of single (oxygen) or three (oxygen, carbon, and nitrogen) atoms present ferromagnetic interactions. We also report a new example of an antiferromagnetic Cu–Gd interaction through the oximato bridge made of two (nitrogen and oxygen) atoms. These experimental observations imply that spin polarization, first expected thirty years ago by Dante et al.,^[1] then retained in recent theoretical calculations, is the mechanism that allows the reproduction of strength and sign of the magnetic Cu–Gd interactions in complexes with Cu and Gd ions. The angular dependence of the ferromagnetic interactions present in simple 3d–Gd complexes, in which the 3d ions have half-occupied 3d_{x²-y²} orbitals, plays in favor of spin-populated 5d Gd orbitals and eliminates the 6s orbital participation. Furthermore the presence of singly occupied 3d_{x²-y²} orbitals is needed for the observation of ferromagnetic 3d Gd interactions, the 3d ions with unoccupied 3d_{x²-y²} orbitals yield antiferromagnetic 3d–Gd interactions. Hence, by

increasing the spin population of the 5d Gd orbitals, the ferromagnetic interaction should increase in 3d-Gd complexes with 3d ions that possess half-occupied $3d_{x^2-y^2}$ orbitals and single-atom bridges.

Acknowledgements

The authors are indebted to Dr. Jean-Paul Malrieu for fruitful discussion. The work was supported by the CNRS, MAGMANet (Grant NMP3-CT-2005-515767).

Keywords: coordination chemistry · Cu–Gd complexes · magnetic properties · spin polarization · structure elucidation

- [1] A. Bencini, C. Benelli, A. Caneschi, R. L. Carlin, A. Dei, D. Gatteschi, *J. Am. Chem. Soc.* **1985**, *107*, 8128–8138.
- [2] C. Benelli, D. Gatteschi, *Chem. Rev.* **2002**, *102*, 2369–2387.
- [3] M. Andruh, J. P. Costes, C. Diaz, S. Gao, *Inorg. Chem.* **2009**, *48*, 3342–3359.
- [4] R. Sessoli, A. K. Powell, *Coord. Chem. Rev.* **2009**, *253*, 2328–2341.
- [5] Y. G. Huang, F. L. Jiang, M. C. Hong, *Coord. Chem. Rev.* **2009**, *253*, 2814–2834.
- [6] H. L. C. Feltham, S. Brooker, *Coord. Chem. Rev.* **2014**, *276*, 1–33.
- [7] J. Paulovic, F. Cimpoesu, M. Ferbinteanu, K. Hirao, *J. Am. Chem. Soc.* **2004**, *126*, 3321–3331.
- [8] J. Cirera, E. Ruiz, *C. R. Chim.* **2008**, *11*, 1227–1234.
- [9] G. Rajaraman, F. Totti, A. Bencini, A. Caneschi, R. Sessoli, D. Gatteschi, *Dalton Trans.* **2009**, 3153–3161.
- [10] S. Kumar Singh, N. Kumar Tibrewal, G. Rajaraman, *Dalton Trans.* **2011**, *40*, 10897–10906.
- [11] S. Kumar Singh, T. Rajeshkumar, V. Chandrasekhar, G. Rajaraman, *Polyhedron* **2013**, *66*, 81–86.
- [12] S. Kumar Singh, G. Rajaraman, *Dalton Trans.* **2013**, *42*, 3623–3630.
- [13] F. Cimpoesu, F. Dahan, S. Ladeira, M. Ferbinteanu, J. P. Costes, *Inorg. Chem.* **2012**, *51*, 11279–11293.
- [14] E. Cremades, S. Gomez-Coca, D. Aravena, S. Alvarez, E. Ruiz, *J. Am. Chem. Soc.* **2012**, *134*, 10532–10542.
- [15] a) V. Gómez, L. Vendier, M. Corbella, J. P. Costes, *Inorg. Chem.* **2012**, *51*, 6396–6404; b) V. Gomez, L. Vendier, M. Corbella, J. P. Costes, *Eur. J. Inorg. Chem.* **2011**, 2653–2656.
- [16] E. Colacio, J. Ruiz, A. J. Mota, M. A. Palacios, E. Ruiz, E. Cremades, M. M. Hänninen, R. Sillanpää, E. K. Brechin, *C. R. Chim.* **2012**, *15*, 878–888.
- [17] a) J. P. Costes, S. Shova, W. Wernsdorfer, *Dalton Trans.* **2008**, 1843–1849; b) J. P. Costes, M. Auchel, F. Dahan, V. Peyrou, S. Shova, W. Wernsdorfer, *Inorg. Chem.* **2006**, *45*, 1924–1934; c) J. P. Costes, F. Dahan, B. Donnadieu, M. J. Rodriguez Douthon, M. I. Fernandez Garcia, A. Bousseksou, J. P. Tuchagues, *Inorg. Chem.* **2004**, *43*, 2736–2744; d) J. P. Costes, F. Dahan, *C. R. Acad. Sci. Ser. IIC* **2001**, *4*, 97–103.
- [18] a) T. Kido, Y. Ikuta, Y. Sunatsuki, Y. Ogawa, N. Matsumoto, *Inorg. Chem.* **2003**, *42*, 398–408; b) Y. Sunatsuki, T. Matsuo, M. Nakamura, F. Kai, N. Matsumoto, J. P. Tuchagues, *Bull. Chem. Soc. Jpn.* **1998**, *71*, 2611–2619.
- [19] a) J. P. Costes, C. Duhayon, S. Mallet-Ladeira, L. Vendier, J. Garcia-Tojal, L. Lopez-Banet, *Dalton Trans.* **2014**, *43*, 11388–11396; b) J. P. Costes, L. Vendier, *C. R. Chim.* **2010**, *13*, 661–667.
- [20] M. F. Richardson, W. F. Wagner, D. E. Sands, *J. Inorg. Nucl. Chem.* **1968**, *30*, 1275–1280.
- [21] S. Sakamoto, T. Fujinami, K. Nishi, N. Matsumoto, N. Mochida, T. Ishida, Y. Sunatsuki, N. Re, *Inorg. Chem.* **2013**, *52*, 7218–7229.
- [22] P. Pascal, *Ann. Chim. Phys.* **1910**, *19*, 5–70.
- [23] A. K. Boudalis, J. M. Clemente-Juan, F. Dahan, J. P. Tuchagues, *Inorg. Chem.* **2004**, *43*, 1574–1586.
- [24] a) J. J. Borrás-Almenar, J. M. Clemente-Juan, E. Coronado, B. S. Tsukerblat, *Inorg. Chem.* **1999**, *38*, 6081–6088; b) J. J. Borrás-Almenar, J. M. Clemente-Juan, E. Coronado, B. S. Tsukerblat, *J. Comput. Chem.* **2001**, *22*, 985–991.
- [25] F. James, M. Roos, *Comput. Phys. Commun.* **1975**, *10*, 343–367.
- [26] STOE: IPDS Manual, version 2.75, Stoe & Cie, Darmstadt (Germany), **1996**.
- [27] Agilent Technologies, Agilent Technologies UK Ltd., Oxford, UK, Xcalibur CCD system, CrysAlisPro Software system, Version 1.171.35.19, **2011**.
- [28] CrysAlis CCD, CrysAlis RED and associated programs, Oxford Diffraction, Oxford Diffraction Ltd, Abingdon (England), **2006**.
- [29] SAINT Bruker, Bruker AXS Inc., Madison, Wisconsin (USA), **2007**.
- [30] SIR92—A program for crystal structure solution: A. Altomare, G. Casciarano, C. Giacovazzo, A. Guagliardi, *J. Appl. Crystallogr.* **1993**, *26*, 343.
- [31] Superflip: L. Palatinus, G. Chapuis, *J. Appl. Crystallogr.* **2007**, *40*, 786–790.
- [32] SHELX97 (Includes SHELXS97, SHELXL97, CIFTAB)—Programs for Crystal Structure Analysis (Release 97–2), G. M. Sheldrick, Institut für Anorganische Chemie der Universität Göttingen (Germany), **1998**.
- [33] CRYSTALS: P. W. Betteridge, J. R. Carruthers, R. I. Cooper, C. K. Prout, D. J. Watkin, *J. Appl. Crystallogr.* **2003**, *36*, 1487.
- [34] WINGX—1.63 Integrated System of Windows Programs for the Solution, Refinement and Analysis of Single-Crystal X-Ray Diffraction Data: L. Farrugia, *J. Appl. Crystallogr.* **1999**, *32*, 837–840.
- [35] *International Tables for X-Ray Crystallography, Vol. IV*, Kynoch Press, Birmingham, **1974**.
- [36] D. J. Watkin, C. K. Prout, L. J. Pearce, *CAMERON Manual*, Chemical Crystallography Laboratory, Oxford (England), **1996**.
- [37] R. Mitsuhashi, T. Suzuki, Y. Sunatsuki, M. Kojima, *Inorg. Chim. Acta* **2013**, *399*, 131–137.
- [38] L. E. Roy, T. Hughbanks, *J. Am. Chem. Soc.* **2006**, *128*, 568–575.
- [39] S. T. Hatscher, W. Urland, *Angew. Chem. Int. Ed.* **2003**, *42*, 2862–2865; *Angew. Chem.* **2003**, *115*, 2969–2971.
- [40] J. P. Costes, J. M. Clemente-Juan, F. Dahan, F. Nicodème, *J. Chem. Soc. Dalton Trans.* **2003**, 1272–1275.
- [41] C. Y. Chow, H. Bolvin, V. E. Campbell, R. Guillot, J. W. Kampf, W. Wernsdorfer, F. Gendron, J. Autschbach, V. Pecoraro, T. Mallah, *Chem. Sci.* **2015**, *6*, 4148–4159.
- [42] J. P. Costes, F. Dahan, A. Dupuis, *Inorg. Chem.* **2000**, *39*, 165–168.
- [43] G. Novitchi, W. Wernsdorfer, L. F. Chibotaru, J. P. Costes, C. E. Anson, A. K. Powell, *Angew. Chem. Int. Ed.* **2009**, *48*, 1614–1619; *Angew. Chem.* **2009**, *121*, 1642–1647.
- [44] E. Colacio, J. Ruiz, A. J. Mota, M. A. Palacios, E. Cremades, E. Ruiz, F. J. White, E. K. Brechin, *Inorg. Chem.* **2012**, *51*, 5857–5868.
- [45] J. P. Costes, F. Dahan, A. Dupuis, J. P. Laurent, *Inorg. Chem.* **1997**, *36*, 4284–4286.
- [46] T. Yamaguchi, J. P. Costes, Y. Kishima, M. Kojima, Y. Sunatsuki, N. Bréfuel, J. P. Tuchagues, L. Vendier, W. Wernsdorfer, *Inorg. Chem.* **2010**, *49*, 9125–9135.
- [47] J. P. Costes, J. M. Clemente-Juan, F. Dahan, F. Dumestre, J. P. Tuchagues, *Inorg. Chem.* **2002**, *41*, 2886–2891.
- [48] J. P. Costes, J. Garcia-Tojal, J. P. Tuchagues, L. Vendier, *Eur. J. Inorg. Chem.* **2009**, 3801–3806.
- [49] E. Colacio, J. Ruiz, G. Lorusso, E. K. Brechin, M. Evangelisti, *Chem. Commun.* **2013**, *49*, 3845–3847.
- [50] T. Birk, K. S. Pedersen, C. A. Thuesen, T. Weyhermüller, M. Schau-Magnussen, S. Pilligkos, H. Weihe, S. Mossin, M. Evangelisti, J. Bendix, *Inorg. Chem.* **2012**, *51*, 5435–5443.
- [51] J. Rinck, Y. Lan, C. E. Anson, A. K. Powell, *Inorg. Chem.* **2015**, *54*, 3107–3117.
- [52] J. P. Costes, J. P. Tuchagues, L. Vendier, J. Garcia-Tojal, *Eur. J. Inorg. Chem.* **2013**, 3307–3311.
- [53] H. Ke, W. Zhu, S. Zhang, G. Xie, S. Chen, *Polyhedron* **2015**, *87*, 109–116.
- [54] T. Terenzio, R. Bastardis, N. Suaud, D. Maynau, J. Bonvoisin, J. P. Malrieu, C. J. Calzado, N. Guihéry, *Phys. Chem. Chem. Phys.* **2011**, *13*, 12314–12320.
- [55] G. Trinquier, N. Suaud, J. P. Malrieu, *Chem. Eur. J.* **2010**, *16*, 8762–8772.
- [56] I. Fernández, R. Ruiz, J. Faus, M. Julve, F. Lloret, J. Cano, X. Ottenwälder, Y. Journaux, C. Munoz, *Angew. Chem. Int. Ed.* **2001**, *40*, 3039–3041; *Angew. Chem.* **2001**, *113*, 3129–3132.
- [57] T. Glaser, H. Theil, M. Heidemeier, *C. R. Chim.* **2008**, *11*, 1121–1136.

Received: October 21, 2015

Published online on January 7, 2016